2024 IEEE International Conference on Robotics and Automation (ICRA 2024)
May 13-17, 2024. Yokohama, Japan

A Novel SEA-based Haptic Interface for Robot-Assisted Vascular Interventional Surgery

Yonggan Yan[1], Shuxiang Guo[1,2,3*], *Fellow, IEEE*, Chuqiao Lyu[1], Jian Guo[3], Jian Wang[3], Pengfei Yang[4], Yongwei Zhang[4], Yongxin Zhang[4], Jianmin Liu[4]

***Abstract*— Robot-assisted vascular interventional surgery can isolate interventionists and X-ray radiation, and improve surgical accuracy. However, the leader side outside the operating room still has problems such as incomplete collection of operating information and unrealistic tactile feedback. The main objective of this paper is to design a haptic interface that can simultaneously capture the force-position information of the interventionists and generate force to assist the interventionists in performing surgeries on the leader side. It can capture the interventionists' delivery displacement, twisting angle, clamping force, and provide real-time force feedback. A leader-follower bidirectional force feedback control strategy was proposed. Based on this strategy, on the one hand, the interventionist perceives the multi-modal information fed back from the follower side, makes judgments, and actively adjusts the surgical operation. On the other hand, the interventionist controls the grasping state of the instruments remotely to control the safety operating force threshold. Finally, the experimental setup was built and a series of evaluation experiments were performed. The experimental results verified the feasibility of the designed haptic interface. It can generate dynamic and accurate force feedback and realize leader-follower grasping force control.**

***Index Terms*— Robot-assisted vascular interventional surgery, force feedback, Leader-follower system, haptic interface.**

I. INTRODUCTION

Cardiovascular and cerebrovascular diseases are the leading cause of death of human beings [1]. Vascular interventional surgery(VIS) has become the main treatment method because of its small trauma [2]. Traditional VIS uses the Digital Subtraction Angiography System(DSA system) to perform imaging of blood vessels and instruments frequently to provide interventionists with information such as vascular lesions and paths. X-ray radiation will be generated during the process, and the accumulated radiation will greatly affect the interventionists' health. Therefore, the VIS robotic system based on the leader-follower structure can isolate the interventionists and radiation in space [3]. The structure of the robot-assisted VIS system is shown in Fig. 1. The left side is the patient side, which includes the DSA system for imaging and a follower robot for reproducing the interventionists' operation. The right side is the surgeon side. The interventionist operates the leader interface outside the operating room by observing the DSA images or video. Surgical information is transmitted between the leader and follower sides remotely. The follower side feeds back information such as images and operating force to interventionists. The leader side transmits control instructions to the follower side, including operating position, operating force, and so on.

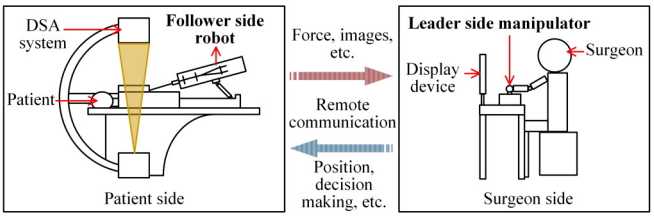

Fig. 1. Control framework of the master-slave VIS robot [3].

The leader side of several commercial VIS robots is usually a combination handle, which lacks tactile feedback [4], [5]. To improve the safety of remote surgery, the haptic interface for VIS robotic system has become a hot research topic. Wang et al. designed a tactile force feedback leader side based on the series elastic actuator(SEA). It can collect the interventionists' delivery displacement and twisting angle, and provide inserting force feedback [6]. Akinyemi et al. proposed a CNN-based hand motion recognition model, which can recognize multiple motions of surgeons' hands [7]. Hooshiar et al. designed a wearable rotation measurement bracelet [8]. Combined with the designed force feedback system based on the magnetic elastomer, the haptic interface can measure operator position and generate force feedback [9]. Based on the viscosity behavior of magnetic fluid under different currents, Guo et al. designed a force feedback method based on magnetic fluid and a non-contact operation measurement method based on photoelectric sensors [10]. Bao et al. designed a haptic interface based on force sensors and magnetic powder brakes to feedback force and torque [11]. However, the existing haptic interfaces for VIS still have the following problems: 1) The leader side only controls the position of the follower robot. The grasping state of surgical instruments is ignored, which is closely related to the contact state between the follower fingers and the instrument.

This work was supported in part by National High-tech Research and Development Program (863 Program) of China (2015AA043202). (Corresponding author: Shuxiang Guo.)

[1]Key Laboratory of Convergence Biomedical Engineering System and Healthcare Technology, The Ministry of Industry and Information Technology, Beijing Institute of Technology, Beijing, 100081, China yanyonggan@bit.edu.cn

[2]The Department of Electronic and Electrical Engineering, Southern University of Science and Technology, Shenzhen, Guangdong 518055,China guo.shuxiang@sustech.edu.cn;

[3]Shenzhen Institute of Advanced Biomedical Robot Co.,Ltd, Shenzhen, China. guojian@abrobo.com;

[4]Neurovascular Center, Changhai hospital, Naval Medical University, Shanghai, China.

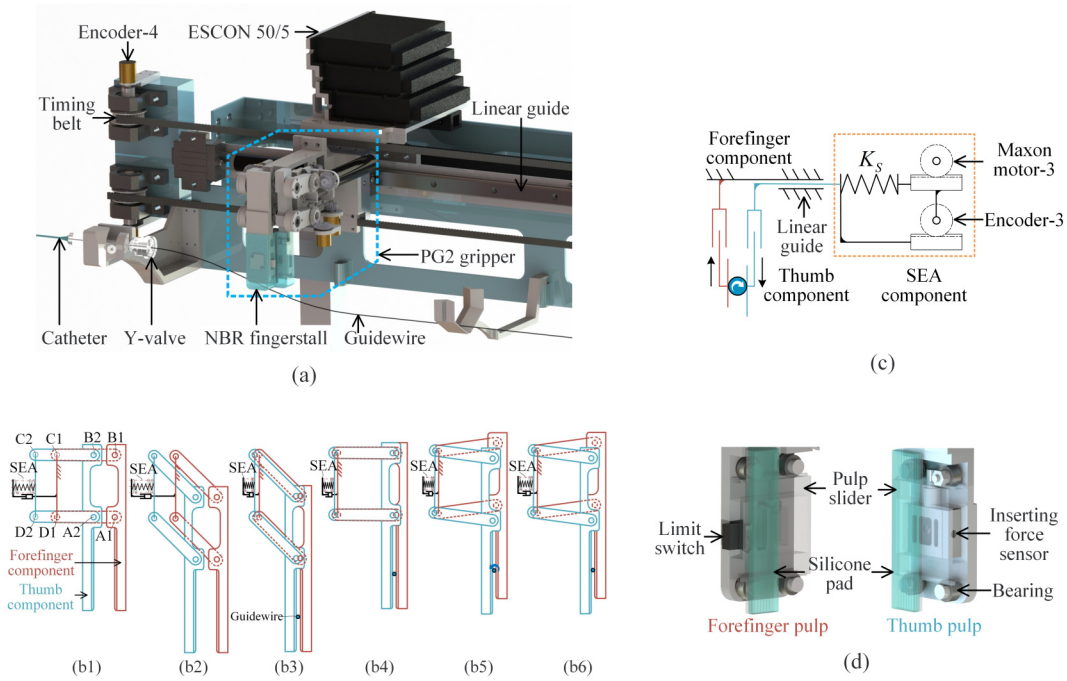

Fig. 2. The follower side. (a) Structure of the follower side. (b1) Opening. (b2) Reaching. (b3) Grasping. (b4) Retreating. (b5) Twisting. (b6) Adjusting grasping force. (c) Schematic diagram of grasping force control. (d) Multifunctional finger pulp mechanism.

2) Most existing haptic interfaces use load cells to measure interactive force and then control motor position or velocity, which risks oscillation under large operating accelerations.

To overcome the existing limitations mentioned above, we propose a novel haptic interface based on SEA. It can not only capture the interventionist's delivery displacement, twist angle and clamping force, but also can generate interactive force through the force feedback control component based on SEA. The operator handles the catheter directly, enabling them to utilize prior accumulated clinical operation experience. Leader-follower bidirectional force feedback is constructed to achieve active and passive safety operations. A series of evaluation experiments were performed to demonstrate the feasibility of the designed haptic interface. It can realize dynamic, stable and accurate tracking of the delivery force and grasping force between leader side and follower side.

The rest of this paper is organized as follows. Section II introduces related work on the follower robot. The mechanical structure and control strategy of the leader side are designed in Section III. Section IV introduces the evaluation experiments. Section V concludes the paper.

II. Related Work

A. Mechanical Structure of the Follower Side

The mechanical structure of the follower side for the VIS is shown in Fig. 2(a), previously designed by the authors [12]. It mainly includes a PG2 gripper that can grasp and twist, and a timing belt component that can insert linearly. PG2 is a parallel gripper with three actuators, which was designed based on two parallelogram mechanisms. It has potential to operate thin catheters and guidewires. By combining the motion space of two fingers, the dexterous operations is performed including opening, reaching, grasping, retracting, twisting, adjusting grasping force, etc., as shown in Fig. 2 (b1-b6). The fingers can be opened to hold instruments of different diameters (0.2-10mm). Similar to the human forefinger and thumb, the two fingers move in the same direction to reach and retract, and move in opposite directions to twist. The instrument is inserted by a motor driving a timing belt that is firmly connected to the gripper. The inserting displacement closed loop is established based on an encoder, and the average inserting accuracy is 0.0848mm.

B. Operation Force in Follower Side

The follower side can accurately measure the grasping force and inserting force. The schematic diagram of measuring and controlling the grasping force between fingers is shown in Fig. 2(c). The SEA component consists of a maxon motor, an encoder, and an elastic component. The elastic force of the elastic component is equal to the grasping force of the instrument. The SEA component controls the compression of the elastic component to adjust the grasping force. The designed multifunctional finger pulp mechanism is shown in Fig. 2(d). Since the forefinger pulp is free in the axial direction of the instrument, the force sensor embedded in the thumb pulp directly measures the inserting force of the instrument. The limit switch installed on the forefinger pulp is used to perceive the instrument sliding between the fingers. The sliding state can provide important information for surgical safety.

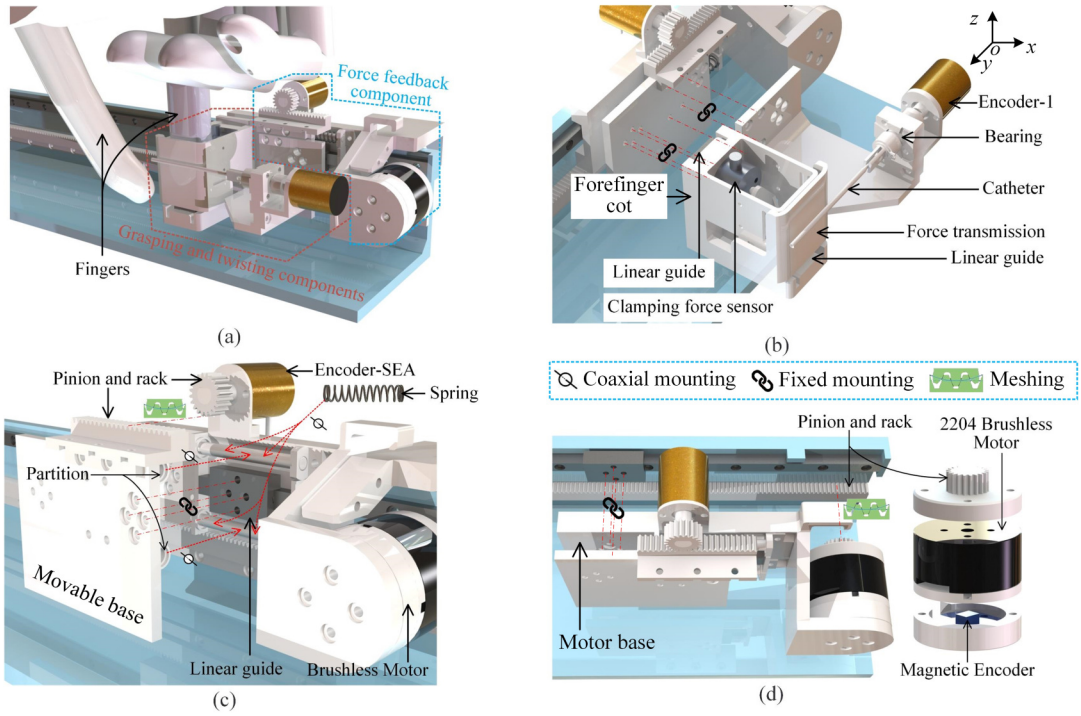

Fig. 3. Structure of the designed haptic interface. (a) The haptic interface includes two components: the force feedback component and the grasping and twisting component. (b) Grasping and twisting component. (c) SEA-based force feedback component. (d) Delivery displacement measurement.

III. Leader Side Developed

A. Mechanical Structure of the Leader Side

As introduced in Section I, the leader side of the VIS robot system is an interactive device used by interventionists to remotely control the follower side in the operating room. It needs to capture the interventionists' operation in real-time, mainly including clamping and releasing, delivery and twisting. To solve the existing problems of incomplete collection of operation information and unrealistic tactile generation, we designed a novel haptic interface for the VIS. The mechanical structure is shown in Fig. 3. The haptic interface mainly includes two components: the grasping and twisting component and the force feedback component, as shown in the red and blue dotted boxes in Fig. 3(a) respectively. The grasping and twisting component is designed to capture operations such as clamping, releasing, and twisting. The force feedback component is used to capture the delivery displacement and generate force feedback to the operator's hand.

The structure of the grasping and twisting component is shown in Fig. 3(b). To capture the clamping force and retain the interventionist's prior clinical operating experience as much as possible, it is designed as a finger cot with a real catheter as the operating handle. A clamping force sensor (SBT674-19.6N, SIMBATOUCH, China) is embedded in the back of the finger cot to measure the clamping force between the operator's thumb and forefinger. Between the two fingers are the forefinger cot, force transmission and catheter. The force transmission part is slidingly connected to the forefinger cot through a linear guide. The clamping force is transmitted by the force transmission and measured by a force sensor. The back of the forefinger cot is slidingly connected to the movable base through a linear guide, which has a degree of freedom(DoF) in the z-axis direction. The DoF is used to compensate for the movement of the catheter in the z-axis direction caused by twisting. The catheter is coaxially connected to the shaft of the encoder-1 through a coupling that is firmly connected to the inner ring of the bearing. The twist angle of the catheter is measured by the 14-bit absolute encoder (1505, RoboBrain, China).

The measurement and generation of interactive force is an important research direction of the haptic interface. Surgeons perceive the excessive operating force of instruments remotely through the force feedback generated by the leader haptic interface, which is important to ensure surgical safety. In addition, experienced surgeons perceive the operating force and perform more effective approach operations. SEA can perform better control in human-robot interaction. It has mechanical compliance, force-sensing capability, and programmable force controllability. Various mechanical or mechatronic systems have adopted SEAs, especially advanced robots like wearable exoskeletons [13]. The designed force feedback component based on SEA can measure and generate the operator's delivery force. The mechanical structure is shown in Fig. 3(c). The elastic elements used in SEA are four standard springs. Four springs and the protruding flanges on the movable base are coaxially mounted on the upper and lower limit columns. On each limiting column, two springs are located on both sides of the movable base

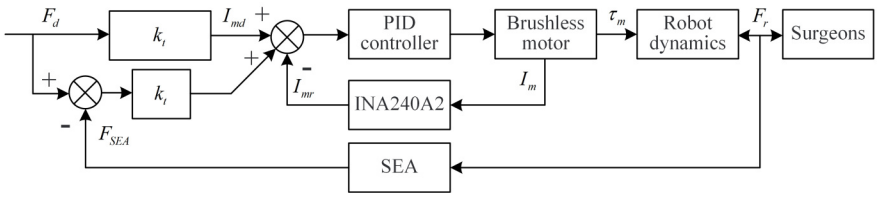

Fig. 4. Control diagram of the leader side. Where F_d represents the desired force, that is, the feedback force. F_r represents the interactive force with the surgeon's hand, F_{SEA} represents the force captured by SEA component, I_m represents the current of the brushless motor, I_{mr} represents the current detected by the INA240A2, τ_m represents the output torque of the motor, k_t represents the brushless motor torque coefficient.

flange and have a certain amount of pre-compression. The two limit blocks resist the right end of the spring group. The movable base and the motor base are slidingly connected along the push-pull direction through a linear guide. Four springs installed symmetrically avoid moments on the linear guide. A rack is fixed with the top of the movable base, which meshes with the gear at the shaft end of the encoder-SEA (1505, RoboBrain, China). The encoder-SEA measures the relative displacement of the movable base and the motor base through the rack and pinion mechanism, that is, the deformation of the spring group. When the motor base is fixed and the external force is applied to the movable base, the movable base deforms the spring group through the flange. The force relationship between the movable base and the motor base can be obtained by calculation. Assuming that the elastic coefficient k_1 of the four springs is the same, then the elastic stiffness k_s of the spring group can be written as:

$$k_s = 4k_1 \tag{1}$$

Assuming that the angle measured by the SEA encoder is θ_s, and the radius of the gear indexing circle is r_s, then the force F_h exerted on the movable base can be expressed as:

$$F_h = k_s \theta_s r_s \tag{2}$$

A brushless motor (BDUAV-2204, China) generates force feedback to the surgeon through a pinion and rack mechanism, as shown in Fig. 3(d). A 12-bit magnetic encoder is installed at the end of the motor stator to capture the rotation angle. Assuming that the motor rotation angle is θ_m, and the gear indexing circle radius is r_m, then the delivery displacement x_m can be calculated as:

$$x_m = \theta_m r_m \tag{3}$$

The direction and value of the operating force exerted by human hands on interactive devices are highly random. Therefore, to ensure that the finger cot can be pushed and pulled freely, especially under high acceleration, the brushless motor is set in the current loop control mode. It avoids the impact on the human hand feedback force due to the position control adjustment process, improving force feedback accuracy and robustness. As shown in Fig. 4, a delivery force closed loop based on SEA is established on the leader side. The control system inner loop is the motor current loop. The three-phase voltage of the brushless motor is detected by the current detection sensor (INA240A2, Texas Instruments, USA). Then the current is converted based on Ohm's law to build a current closed loop. The output torque of the brushless motor is converted into the interaction force after being transmitted by the mechanical system. The force is measured by the designed SEA component and differs from the follower feedback force as compensation for the desired motor current. Furthermore, a force feedback closed loop at the leader side is established to provide the operator with the follower force as input.

B. Leader-Follower Bidirectional Force Feedback

Our previous studies have demonstrated the efficiency of the grasping force control in ensuring surgical safety [12], and this conclusion is also applicable in traditional VIS. Further, a leader-follower bidirectional force feedback control strategy was designed, as shown in Fig. 5. There are two transmission routes in opposite directions between the leader side and the follower side. The direction of the red line represents the remote grasping force control. The blue line represents the force feedback from the follower side. Appropriate grasping force control at the follower side can ensure the safety threshold of insertion force. This value can be controlled by experienced interventionists on the leader side. The novices can use the grasping force autonomous control method mentioned in the study [12]. Grasping force control is key to realizing passive safety because the controlled inserting force threshold is determined by the friction state between the gripper and the instrument. The haptic feedback generated by the leader side for the operator affects the operator's decision-making and operation, which is defined as an active safety strategy. By reproducing the follower side operating state, the leader side enables the operator to perceive states where the instrument is blocked in the body, entering undesired bifurcation, etc. Compared with the passive safety method, the active safety method relies on the operator's decision-making, the calculation of the system program, the measurement of sensor information, etc., resulting in slightly lower real-time performance, but stronger functionality. The two safety methods compensate each other to improve the safety of robot-assisted VIS.

IV. Evaluation and Experiments

A. SEA Calibration

The elastic coefficient of the SEA component was calibrated, and the experimental setup was established as shown in Fig. 6(a). The motor base is fixed. A force sensor is

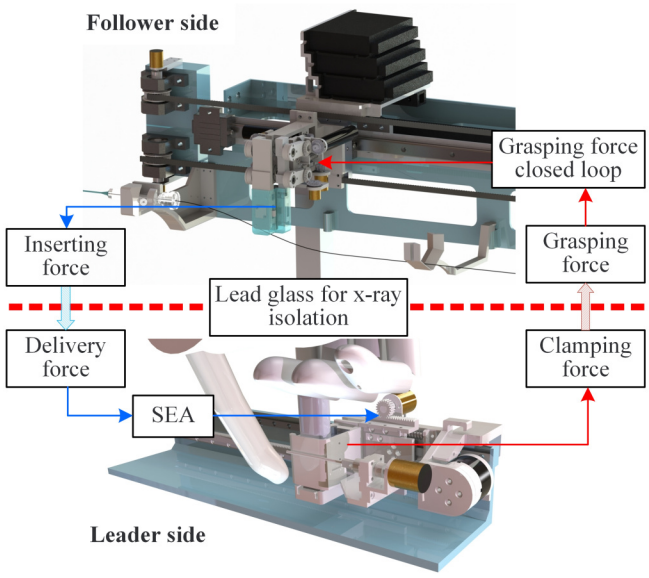

Fig. 5. Leader-follower bidirectional force feedback control strategy. The red line represents the grasping force control. The blue line represents the inserting force feedback.

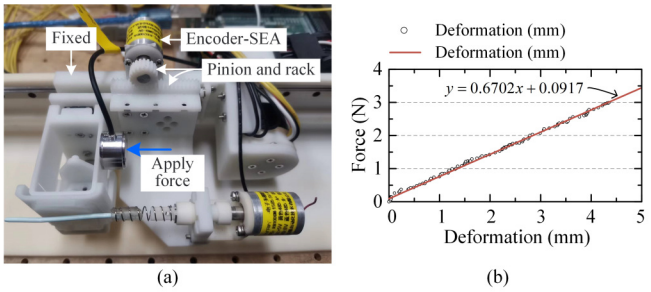

Fig. 6. SEA calibration. (a) Experimental setup for calibration. (b) Calibration experiment results. The fitted elastic coefficient of the spring group $k_s = 0.6702N/mm$. The intercept between the fitting line and the y-axis is not zero because of the friction.

installed on the right side of the forefinger cot, and the direction of applied force is consistent with the direction of SEA compression. The encoder-SEA measures the deformation of the spring group. Gradually applied force (0-3N) on the force sensor and measured the spring group deformation. The calibration experiment results are shown in Fig. 6(b). The black circles represent the measured sample points. The deformation characteristic curve of the spring group was obtained by the least squares fitting, as shown in the red line in Fig. 6(b). The fitting function is:

$$y = 0.6702x + 0.0917 \tag{4}$$

where x represents the spring group deformation, y represents the force measured by the force sensor. The fitted characteristic curve is consistent with the experimental results (Pearson Correlations=0.9986 and Signifcant level: 0.05).

B. Evaluation of Bidirectional Force Feedback

To demonstrate the feasibility of the proposed haptic interface, it was integrated with the follower side, previously

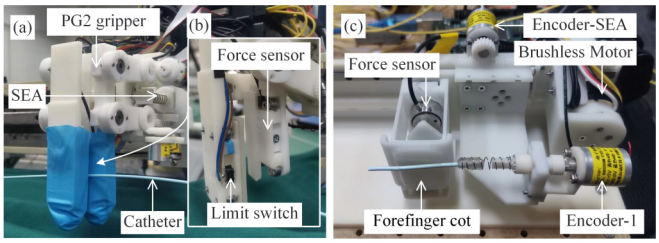

Fig. 7. Experimental setup for the evaluation of bidirectional force feedback. (a) Follower side. (b) Multifunctional finger pulp. (c) Leader side.

developed by the authors [12], as shown in Fig. 7 (a, b). The PG2 gripper can grasp, twist, and insert catheters and guidewires. The designed multifunctional finger pulp structure is shown in Fig. 7(b). The installed limit switch and force sensor are used to measure the sliding state and inserting force of the instrument respectively. SEA components were mounted perpendicular to the grasping surface to flexibly grasp the instruments and adjust the grasping force.

The built leader side haptic interface is shown in Fig. 7(c). Encoder-SEA is used to measure the spring group deformation of SEA, which is converted into interactive force after calculation. The clamping force sensor, mounted on the forefinger cot, measures the clamping force. Encoder-1 measures the twisting angle. A spring is used to connect Encoder-1 and the catheter to reduce the twisting resistance caused by the different axes of the two. On the one hand, the brushless motor measures the delivery displacement through the magnetic encoder. On the other hand, it generates force feedback to the operator through the current closed loop. The actual interactive forces measured by SEA constructed the control outer loop. Combining the outer loop with the motor current loop, the delivery force closed loop was constructed. Due to the randomness of human operation, a PD controller is used to ensure the system response speed.

The delivery force static and dynamic control performance was evaluated through the square wave force signal tracking experiment and the sinusoidal wave force signal tracking experiment. The experimental results of 10 cycles of square waves are shown in Fig. 8(a). The blue dotted line represents the desired signal, the red line represents the tracking results, and the black line represents the error. Square wave signal set period $T = 8s$ and amplitude $A = 0.5N$. After stabilization, the maximum static error was 10mN, and the overall average absolute error was 30.7mN. The sinusoidal wave signal sets the period $T = 10s$ and amplitude $A = 1N$. The dynamic average absolute error was 57.4mN and the root mean square error was 68.8mN. The experimental results showed the feasibility of the proposed haptic interface in generating accurate force feedback.

In the grasping force control evaluation experiment, the operator randomly controlled the clamping force of the catheter multiple times. The leader-follower grasping force tracking experimental results is shown in Fig. 8(c). The blue dotted line represents the leader side clamping force, the red line represents the follower side grasping force, and the

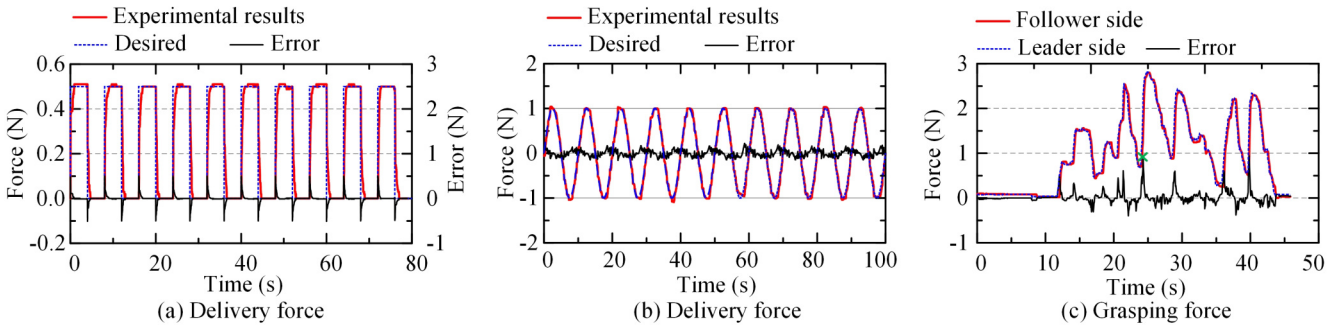

Fig. 8. Evaluation of experimental results for the haptic interface. (a) Square wave signal: $T = 8s$, $A = 0.5N$. (b) Sinusoidal signal: $T = 10s$, $A = 1N$. (c) Grasping force control.

black line represents the error. The average absolute tracking error of the leader-follower grasping force dynamic control was 75.1mN. As shown in Fig. 8(c), the point shown by the green x symbol has a large tracking error. The reason is the delay caused by leader-follower communication and motor drive, and the error is adjusted to a lower level within 0.4s. The experimental results showed that the operator can remotely control the instrument's grasping state to realize safety operations such as passive sliding between fingers.

V. Conclusion

The main objective of this paper is to propose a new SEA-based haptic interface on the leader side, which can capture the interventionist's delivery displacement, twist angle, inserting force, and clamping force. A leader-follower bidirectional force feedback control strategy was proposed. The operator perceives the inserting force feedback from the follower side. Based on its dynamic characteristics, the instrument's state in the blood vessel is then predicted to adjust the surgical operation. Meanwhile, the operator remotely controls the grasping force of the follower robot to adjust the maximum inserting force threshold of the instrument. It can passively ensure operation safety in critical areas. The safety operation strategy that combines active and passive safety methods has the potential to improve safety in remote VIS. Finally, a series of experiments were performed to evaluate the haptic interface, including the leader-follower inserting force tracking experiment and the leader-follower grasping force tracking experiment. Experimental results showed that the designed haptic interface can realize dynamic, stable, and accurate generation of bidirectional force feedback. In the future we will further consider the various disturbance forces of the system to improve the dynamic performance of haptic feedback. The haptic interface will be combined with the follower robot system to conduct *in-vitro* and *in-vivo* experiments.

References

[1] W. H. Organization, "World health statistics 2021: monitoring health for the sdgs, sustainable development goals," World Health Organization, Tech. Rep., 2020.

[2] P. Shi, S. Guo, L. Zhang, X. Jin, H. Hirata, T. Tamiya, and M. Kawanishi, "Design and evaluation of a haptic robot-assisted catheter operating system with collision protection function," *IEEE Sensors Journal*, vol. 21, no. 18, pp. 20 807–20 816, 2021.

[3] Y. Yan, S. Guo, C. Lyu, D. Zhao, and Z. Lin, "A novel steerable catheter for vascular interventional surgery," in *2023 IEEE International Conference on Mechatronics and Automation (ICMA)*. IEEE, 2023, pp. 766–771.

[4] E. Durand, R. Sabatier, P. C. Smits, S. Verheye, B. Pereira, and J. Fajadet, "Evaluation of the r-one robotic system for percutaneous coronary intervention: the r-evolution study," *EuroIntervention: journal of EuroPCR in collaboration with the Working Group on Interventional Cardiology of the European Society of Cardiology*, vol. 18, no. 16, pp. e1339–e1347, 2023.

[5] C. Beaman, H. Saber, and S. Tateshima, "A technical guide to robotic catheter angiography with the corindus corpath grx system," *Journal of NeuroInterventional Surgery*, vol. 14, no. 12, pp. 1284–1284, 2022.

[6] K. Wang, X. Mai, H. Xu, Q. Lu, and W. Yan, "A novel sea-based haptic force feedback master hand controller for robotic endovascular intervention system," *The International Journal of Medical Robotics and Computer Assisted Surgery*, vol. 16, no. 5, pp. 1–10, 2020.

[7] T. O. Akinyemi, O. M. Omisore, W. Du, W. Duan, X. Chen, G. Yi, and L. Wang, "Interventionalist hand motion recognition with convolutional neural network in robot-assisted coronary interventions," *IEEE Sensors Journal*, 2023.

[8] A. Hooshiar, A. Sayadi, J. Dargahi, and S. Najarian, "Integral-free spatial orientation estimation method and wearable rotation measurement device for robot-assisted catheter intervention," *IEEE/ASME Transactions on Mechatronics*, vol. 27, no. 2, pp. 766–776, 2021.

[9] A. Hooshiar, A. Payami, J. Dargahi, and S. Najarian, "Magnetostriction-based force feedback for robot-assisted cardiovascular surgery using smart magnetorheological elastomers," *Mechanical Systems and Signal Processing*, vol. 161, p. 107918, 2021.

[10] S. Guo, Y. Song, X. Yin, L. Zhang, T. Tamiya, H. Hirata, and H. Ishihara, "A novel robot-assisted endovascular catheterization system with haptic force feedback," *IEEE Transactions on Robotics*, vol. 35, no. 3, pp. 685–696, 2019.

[11] X. Bao, S. Guo, C. Yang, and L. Zheng, "Haptic interface with force and torque feedback for robot-assisted endovascular catheterization," *IEEE/ASME Transactions on Mechatronics*, 2023.

[12] Y. Yan, S. Guo, Z. Lin, C. Lyu, D. Zhao, P. Yang, Y. Zhang, Y. Zhang, and J. Liu, "Grasping force-based passive safety method for a vascular interventional surgery robot system," *IEEE Transactions on Instrumentation and Measurement*, 2023.

[13] S. Han, H. Wang, Y. Tian, and H. Yu, "Enhanced extended state observer-based model-free force control for a series elastic actuator," *Mechanical Systems and Signal Processing*, vol. 183, p. 109584, 2023.